CRYSTALLIZATION OF A MELT SPUN Fe–Ni BASED METALLIC GLASS

J. J. Suñol[1*]*, M. T. Clavaguera-Mora*[2] *and N. Clavaguera*[3]

[1]Department of Physics, EPS (P II), Universitat de Girona, 17071 Girona, Spain
[2]Department of Physics, Facultat de Ciències, Universitat Autònoma de Barcelona, 08193 Bellaterra, Spain
[3]Department of ECM, Facultat de Física, Universitat de Barcelona, 08028 Barcelona, Spain

Abstract

The crystallization kinetics of a melt spun Fe–Ni based alloy has been investigated, with both isothermal and continuous heating experiments, by means of differential scanning calorimetry. The alloy presents two separated crystallization processes. In order to perform the kinetic analysis of a melt spun metallic glass and to decide which kinetic model agrees better with the experimental crystallization data as the crystallized fraction x. We compare the experimental dependence of $\ln(k_0 f(x))$ *vs.* $(1–x)$ and that predicted, assuming different model equations for $f(x)$. Both crystallization processes follow the JMAE equation and the master curve is the same for isothermal and non-isothermal data.

Keywords: crystallization, DSC, metallic glass

Introduction

A detailed knowledge of the temperature dependence of nucleation and growth is essential for materials design, since these processes controls the phases and microstructure formed. Moreover, in technical applications, the thermal stability of metallic glasses is a problem of fundamental interest because the useful working temperature ranges will de determined by the structural changes and eventual crystallization occurring at the operating temperature. Furthermore, kinetic investigations of the crystallization of glass are of interest for understanding the nature of processes of glasses. One of the common, and perhaps least cumbersome, experimental methods of obtaining the kinetic behavior is through the use of thermoanalytical techniques as differential thermal analysis (DTA) or differential scanning calorimetry (DSC) [1–5].

The field of rapid solidification of metals and alloys from the liquid state has undergone enormous progress during the last decades. This started with the successful rapid quenching experiments of Falkenhagen [6] and Duwez [7, 8], where different extended solid solutions were obtained. A large number of metastable materials, such as amorphous phases, extended solid solutions and non-equilibrium crystalline phases, have been produced. As an example, it is known that Fe-based alloys pre-

---

* Author for correspondence: E-mail: joanjosep.sunyol@udg.es

pared by rapid solidification techniques in ribbon form exhibit superior soft magnetic properties [9]. In this work, a melt spun Fe–Ni based metallic glass was obtained and their crystallization kinetics analyzed by means of calorimetry experiments.

Experimental details

In this work, the Fe–Ni based alloy was obtained by rapid solidification, i.e., melt spinning. The precursors used were mixed and pressed powders of elemental Fe, Ni, Si, P and Fe_3P (to prevent P sublimation). The quaternary alloy analyzed is chosen to be 80% metal–20% metalloid. The nominal composition of the metallic glass ribbons studied was: $Fe_{40}Ni_{40}P_{12}Pi_8$. Pure elements and compound (<99.9 at.%) and small particle sizes were chosen (smaller than 20 μm) as precursors. The melt spinning process was performed in a conventional laboratory device working in the optimal conditions to obtain an amorphous alloy [10]. The ribbon was produced, by quenching the molten alloy on the surface of a rapidly spinning (about 32 m s^{-1}) Cu wheel. The working atmosphere was inert, Ar. The ribbon was about 0.30 cm wide and 35 μm thick as measured by scanning electron microscopy (SEM) observations performed in a Zeiss DSM960A apparatus.

Differential scanning calorimetry (DSC) was done with an argon purging gas. The DSC machine used is the Perkin Elmer DSC7. These measurements were necessary for the study of the crystallization behavior of the melt-spun ribbons in the case of an amorphous phase. Thermal stability was analyzed via isothermal and non-isothermal experiments. The scanning rates employed varied from 5 to 40 K min^{-1}. The calorimetric experiments were carried out in a DSC7 Perkin Elmer calorimeter under an inert argon atmosphere. Isothermal measurements were performed at a heating rate of 300 K min^{-1} until the annealing temperature was reached. The isothermal temperatures were selected below the onset temperatures of the crystallization processes.

Results and analysis

The amorphous state of the non-treated ribbon was demonstrated by X-ray diffraction and Transmission Mössbauer spectroscopy similarly to [11]. Furthermore, the chemical composition of the previously powdered ribbon was analyzed with the induced coupled plasma (ICP) technique. As expected, the results show that the final composition is close to the original [12]. The ribbon topology was examined by SEM. As an
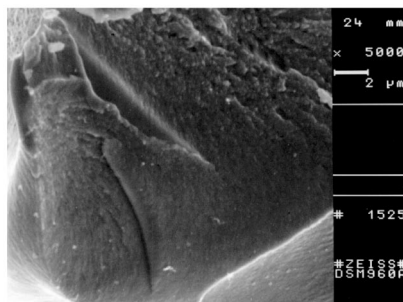

Fig. 1 SEM micrograph of a fractured ribbon

example, Fig. 1, that corresponds to a fractured zone. SEM resolution was 3.5 nm, acceleration voltage was 15 kV, and working distance was between 11 and 24 mm. Samples had been sputtered previously with K 550 Emitech equipment.

The DSC scans under continuous heating conditions show the presence of two exothermic peaks, labeled as A and B respectively, associated to a main crystallization at low temperature and to a secondary reordering and crystallization of the remaining amorphous phase the high temperature small process. As an example, Fig. 2. Furthermore, several isothermal measurements were performed (Fig. 3 for main crystallization peak).
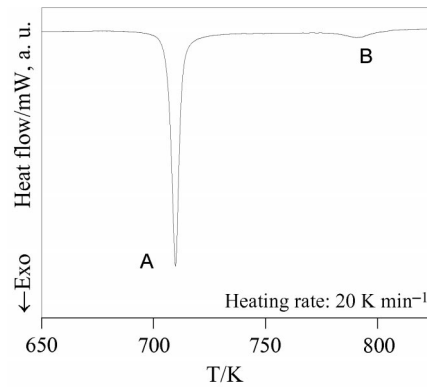

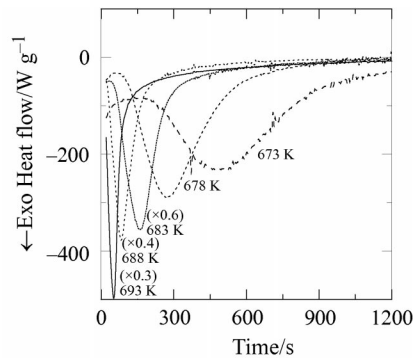**Fig. 2** DSC scan at continuous heating rate (20 K min^{-1}) of the melt-spun alloy Fe$_{40}$Ni$_{40}$P$_{12}$Si$_8$

Fig. 3 DSC isothermal scans at different isothermal temperatures of the main crystallization process of the melt-spun alloy Fe$_{40}$Ni$_{40}$P$_{12}$Si$_8$

From the experimental data, the kinetic analysis was performed. To explain the thermal behavior of the glasses upon crystallization, we assume a rate of reaction given by

$$\frac{dx}{dt} = k(T)f(x) \tag{1}$$

where x is the crystallized fraction at time, t, and temperature, T, $k(T)$ is the rate constant and $f(x)$ is a function that reflects the mechanism of crystallization. These two functions are assumed to be independent of the thermal history of the sample, with an Arrhenius form of the rate constant, under both isothermal and continuous heating conditions. To check the validity of the method irrespective of the experimental procedure (isothermal or continuous heating) a usual graph method is the plot of $\ln(dx/dt)$ *vs.* $1/T$ [13].

Once the value of the apparent activation energy is known, the function $f(x)$ can be evaluated from the continuous heating and from isothermal experiments. If the kinetic behavior is the same in both kind of experiments, the experimentally measured $\ln(k_0 f(x))$ *vs.* $\ln(1-x)$ has to be independent of heating rate and identical to that obtained in an isothermal regime. That expression can be evaluated from dx/dt by taking

$$\ln(k_0 f(x)) = \ln\left(\frac{dx}{dt}\right) - \frac{E}{RT} \qquad (2)$$

where k_0 is a constant parameter and E the apparent activation energy. These parameters are characteristic the Arrhenius equation.

Furthermore, the analysis of the function $f(x)$ is useful if we want to distinguish which one of the several existing kinetic models can best describe the crystallization process. All measured DSC curves for every crystallization stage can be directly compared.

In order to perform the kinetic analysis and to decide which kinetic model agrees better with our experimental crystallization data as the crystallized fraction x. We compare the experimental dependence of $\ln(k_0 f(x))$ *vs.* $\ln(1-x)$ and that predicted, assuming different model equations for $f(x)$. This or other equivalent graphs were used by several authors [14–15].

The apparent activation energies, E, can be obtained with several techniques as the Kissinger [16] or the Ozawa [17] methods. Nevertheless, as well known these methods use logarithm linearization and not consider all data from DSC measurements. For that reason they are very sensitive to the experimental errors. Several more complex methods can be applied to obtain the activation energy. In our work, the isoconversional method developed by Málek [18–20] is applied to obtain the E value from non-isothermal DSC scans at several heating rates in the crystallization process of the Fe–Ni based alloy produced by rapid solidification. In the central zone ($0.20 < x < 0.70$) the E values are 3.5 ± 0.2 and 4.1 ± 0.2 eV for the main and secondary crystallization process, respectively.

The kinetic model that gives the best fit to our experimental data in the two stages of crystallization of both alloys can be unambiguously represented by the Johnson–Mehl–Avrami–Erofe'ev (JMAE) equation $f(x) = n(1-x)(-\ln(1-x))^{(n-1)/n}$ where n is the kinetic exponent.

In the first crystallization process (A), the experimental data follows one master curve as shown in Fig. 4. Although there is a certain degree of dispersion of the points in several cases, the overall pattern is sufficiently good to justify the use of JMAE equation to study the crystallization kinetics of this metallic glass. Furthermore, the master curve is the same for isothermal and non-isothermal data. We can state that the
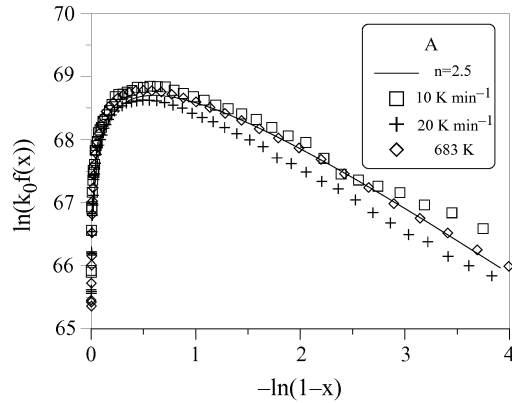
Fig. 4 Plot of $\ln(k_0 f(x))$ *vs.* $-\ln(1-x)$ for the low temperature crystallization process, A. Symbols represent experimental data ($\square$ – 10 K min^{-1} heating rate, $+$ – 20 K min^{-1} heating rate and $\diamond$ – isothermal annealing at 683 K) and lines give the theoretical plot

crystallization mechanism is the same for isothermal and non-isothermal conditions. The 2.5 value of the *n* parameter corresponds to a three-dimensional volume growth controlled by diffusion [21].

In the second crystallization process (B), the value of its kinetic exponent is not constant, as shown in Fig. 5. In the nearly stages, *n* changes steeply revealing the transient nucleation effect to reach values corresponding to a three-dimensional volume growth controlled by diffusion in the central part (0.20<*x*<0.55). Latter in the transformation *n* continuously decreases. Really, the *n* value changes continuously as a function of transformed fraction. In the nearly stages, *n* changes steeply revealing the transient nucleation effect to reach the value ranging of 1.6 in the central part of the transformation (0.20<*x*< 0.55). Latter in the transformation *n* continuously decreases
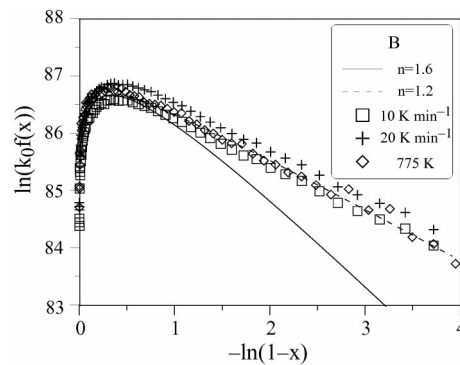

Fig. 5 Plot of $\ln(k_0 f(x))$ *vs.* $-\ln(1-x)$ for the high temperature crystallization process, B. Symbols represent experimental data ($\square$ – 10 K min^{-1} heating rate, $+$ – 20 K min^{-1} heating rate and $\diamond$ – isothermal annealing at 775 K) and lines give the theoretical plot

to 1.2. One possible cause is the influence of a second crystallization step, as detected in FeSiB glassy ribbons [22], but in our case both crystallization process are clearly differentiated. The most probable is that the n decrease reflects the saturation of nucleation [23]. Moreover, this complicated behavior is not surprising since not only nucleation and crystal growth but also change of composition of the crystalline phase can occur. To draw more valuable scientific conclusions it is necessary to extent the analysis to more compositions and the use of structural techniques.

Conclusions

An Fe–Ni based quaternary glassy alloys were obtained by melt spinning: $Fe_{40}Ni_{40}P_{12}Si_8$. The alloy presents two stages of crystallization well separated in temperature. The apparent activation energies, E, are obtained by the isoconversional method developed by Málek from non-isothermal DSC scans at several heating rates. In the central zone ($0.20 < x < 0.70$) the E values are 3.5±0.2 and 4.1±0.2 eV respectively.

Although there is a certain degree of dispersion, the kinetic model that gives the best fit of the experimental data in the two stages of crystallization is the Johnson–Mehl–Avrami–Erofe'ev (JMAE) equation. In the low temperature crystallization process, all data follow one master curve. Furthermore, the value of its JMAE kinetic exponent is constant. The 2.5 value corresponds to a three-dimensional volume growth controlled by diffusion. Nevertheless, in the high temperature crystallization process the JMA kinetic exponent is not constant. In the nearly and central stages, n changes steeply revealing the transient nucleation effect to reach in the central part a value corresponding to growth controlled by diffusion. Latter in the transformation n continuously decreases reflecting the saturation of nucleation.

* * *

References

 1 T. Ozawa, Polymer, 12 (1971) 150.
 2 J. Zhu, Z. Bo and D. Dong, J. Non-Cryst. Solids, 201 (1996) 47.
 3 C. Y. Li, D. Yan, S. Z. D. Cheng, F. Bai, J. J. Ge, B. H. Calhoun, T. He, L.-C. Chien,
    F. W. Harris and B. Lotz, Phys. Rev. B, 60–18 (1999) 12675.
 4 C. Basire and D. A. Ivanov, Phys. Rev. Letters, 85–26 (2000).
 5 J. J. Suñol, M. T. Clavaguera-Mora and N. Clavaguera, J. Therm. Anal. Cal., 70 (2002) 173.
 6 G. Falkenhagen and W. Hoffman, Z. Metallk., (1952) 69.
 7 P. Duwez, R. H. Willens and W. Klement, J. Appl. Phys., (1960) 1136.
 8 P. Duwez, W. Klement and R. H. Willens, Nature, 186 (1960) 869.
 9 K. Suzuki, J. Met. Nanocryst. Mater., 2 (1999) 3.
10 J. J. Suñol, N. Clavaguera and M. T. Mora, J. Therm. Anal. Cal., 52 (1998) 853.

11 T. Pradell, J. J. Suñol, N. Clavaguera and M. T. Clavaguera-Mora, J. Non-Cryst. Solids, 276 (2000) 113.

12 J. J. Suñol, Ll. Escoda, J. Saurina and J. Caleya. XXVIII Reunión bienal de la RSEF, Sevilla 2001, p. 324.

13 S. Bordas, M. T. Clavaguera-Mora and N. Clavaguera, J. Non-Cryst. Solids, 119 (1990) 232.

14 S. Suriñach, M. D. Baró, J. A. Diego, M. T. Clavaguera-Mora and N. Clavaguera. Acta Metall. Mater., 40 (1992) 37.

15 I. Mat'ko, E. Illekova, P. Svec, P. Duhaj and K. Czomorova, Mater. Sci. Eng. A, 226–228 (1997) 280.

16 H. E. Kissinger, Anal. Chem., 29 (1957) 1702.

17 T. Ozawa, Bull. Chem. Soc. Japan., 38 (1965) 1881.

18 J. M. Criado, J. Málek and A. Ortega, Thermochim. Acta, 147 (1989) 377.

19 J. Málek, Thermochim. Acta, 200 (1992) 257.

20 J. Málek, Thermochim. Acta, 267 (1995) 61.

21 J. W. Christian, in 'Theory of transformation of metals and alloys'. Ed. Pergamon, Oxford 1975, Chap. 12.

22 I. Mat'ko, E. Illekova, P. Svec and P. Duhaj, Mater. Sci. Eng. A, 225 (1997) 145.

23 M. T. Clavaguera-Mora, S. Suriñach, M. D. Baró and N. Clavaguera, J. Mater. Sci., 18 (1983) 1381.